arXiv:1905.10138v1 [cs.LG] 24 May 2019

Structured Compression by Unstructured Pruning for Sparse Quantized Neural Networks

Se Jung Kwon[*1], **Dongsoo Lee**[*1], **Byeongwook Kim**[1], **Parichay Kapoor**[1]
Baeseong Park[1], **Gu-Yeon Wei**[1,2]
[1]Samsung Research, Seoul, Republic of Korea
[2]Harvard University, Cambridge, MA
{sejung0.kwon, dongsoo.lee3, byeonguk.kim, pk.kapoor,
bpbs.park, gy.wei}@samsung.com

Abstract

Model compression techniques, such as pruning and quantization, are becoming increasingly important to reduce the memory footprints and the amount of computations. Despite model size reduction, achieving performance enhancement on devices is, however, still challenging mainly due to the irregular representations of sparse matrix formats. This paper proposes a new representation to encode the weights of Sparse Quantized Neural Networks, specifically reduced by find-grained and unstructured pruning method. The representation is encoded in a structured regular format, which can be efficiently decoded through XOR gates during inference in a parallel manner. We demonstrate various deep learning models that can be compressed and represented by our proposed format with fixed and high compression ratio. For example, for fully-connected layers of AlexNet on ImageNet dataset, we can represent the sparse weights by only 0.09 bits/weight for 1-bit quantization and 91% pruning rate with a fixed decoding rate and full memory bandwidth usage.

1 Introduction

Deep neural networks (DNNs) are evolving to solve increasingly complex and varied tasks with dramatically growing data size [7]. As a result, the growth rate of model sizes for recent DNNs leads to slower response times and higher power consumption during inference [10]. To mitigate such concerns, model compression techniques have been introduced to significantly reduce model size of DNNs while maintaining reasonable model accuracy [7].

It is well known that DNNs are designed to be over-parameterized in order to ease local minima exploration [6, 15]. Thus, various model compression techniques have been proposed for high-performance and/or low-power inference. For example, pruning techniques remove redundant weights (to zero) without compromising accuracy [19], in order to achieve memory and computation reduction on devices [9, 28, 39, 22]. As another model compression technique, non-zero weights can be quantized to fewer bits with comparable model accuracy of full-precision parameters, as discussed in [5, 30, 14, 34].

To achieve even higher compression ratios, pruning and quantization can be combined to form Sparse Quantized Neural Networks (SQNNs). Intuitively, quantization can leverage parameter pruning since pruning reduces the number of weights to be quantized and quantization loss decreases accordingly [20]. Deep compression [11], trained weight networks (TWN) [24], trained ternary

[*]Equal contribution.

Preprint. Under review.

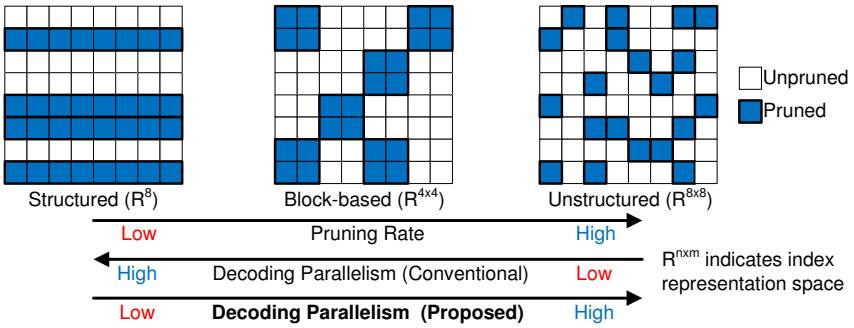

Figure 1: Several types of pruning granularity. In the conventional sparse formats, as a sparse matrix becomes more structured to gain parallelism in decoding, pruning rate becomes lower in general.

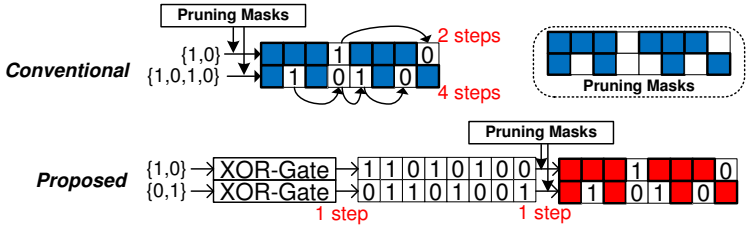

Figure 2: Comparison between conventional and proposed sparse matrix decoding procedures given a pruning mask. In the conventional approach, the number of decoding steps for each row can be different (i.e., degraded row-wise parallelism). On the contrary, the proposed approach uses XOR-gate decompressors and decodes each row at one step.

quantization (TTQ) [38], and viterbi-based compression [1, 21] represent recent efforts to synergistically combine pruning and quantization.

To benefit from sparsity, it is important to (1) represent pruned models in a format with small memory footprint and (2) implement fast computations based on a sparse matrix. Even if reduced SQNNs can be generated with a high pruning rate, it is challenging to gain performance enhancement without an inherently parallel sparse-matrix decoding process during inference. Structured and blocked-based pruning techniques [25, 2, 36, 13, 35] for DNNs have been proposed to accelerate decoding of sparse matrices using reduced indexing space, as Figure 1 shows. However, coarse-grained pruning associated with reduced indexing space exhibits relatively lower pruning rates compared to unstructured pruning [26], which masks weights randomly with fine-grained granularity. In conventional sparse matrix formats, due to random locations of weights to be pruned, decoding time can vastly differ if decoding processes are conducted in different blocks simultaneously, as shown in the conventional approach of Figure 2.

To enable inherently parallel computations using sparse matrices, this paper proposes a new sparse format. Our main objective is to remove all pruned weights such that the resulting compression ratio tracks the pruning rate, while maintaining a regular format. Interestingly, in VLSI testing, proposals for test-data compression have been developed from similar observations, i.e., there are lots of *don't care* bits (= pruned weights in the case of model compression) and the locations of such *don't care* bits seem to be random [32] (the locations of unstructurally pruned weights also seem to be random). We adopt XOR gates, previously used for test-data compression, to decode the compressed bits in a fixed rate during inference, as shown in Figure 2. XOR gates are small enough such that we can embed multiple XOR gates to fully utilize memory bandwidth and decode many sparse blocks concurrently. Correspondingly, we propose an algorithm to find encoded and compressed data to be fed into XOR gates as inputs.

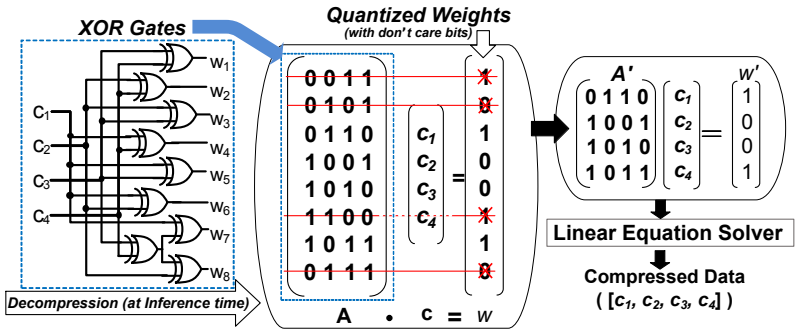

Figure 3: Given a fixed matrix $\boldsymbol{A}$ representing the structure of XOR gates, compressing $\boldsymbol{w}$ is to solve $\boldsymbol{Ac} = \boldsymbol{w}$ and the decompression is to calculate the product of $\boldsymbol{A}$ and $\boldsymbol{c}$ over $GF(2)$. To find $\boldsymbol{c}$ satisfying $\boldsymbol{Ac} = \boldsymbol{w}$, we solve reduced linear equations after removing equations with *don't care* bits. Once $\boldsymbol{c}$ is obtained, *don't care* bits are randomly filled by XOR gates during decompression as byproducts.

2 Compressed and Structural Representation

Test-data compression usually generates random numbers as outputs using the input data as seed values. The outputs (test data containing *don't care* bits) can be compressed successfully if such outputs can be generated by the random number generator using at least one particular input seed data (which is the compressed test data). It is well known that memory reduction can be as high as the portion of *don't care* bits [3, 32] if randomness is good enough. Test data compression and SQNNs with fine-grained pruning share the following properties: 1) Parameter pruning induces *don't care* values as much as pruning rates and 2) If a weight is unpruned, then each quantization bit is assigned to 0 or 1 with equal probability [1].

2.1 Compression and Decompression with XOR gates

We use an XOR-gate network as a random number generator due to its simple design and strong compression capability (such a generator is not desirable for test-data compression because it requires too many input bits). Suppose that a real-number weight matrix $\boldsymbol{W}$ is quantized to be binary matrices $\boldsymbol{W}_i^q$ $(1 \leq i \leq n_q)$ with n_q as the number of bits for quantization. As the first step of our compression algorithm, we reshape each binary matrix $\boldsymbol{W}_i^q$ to be a 1D vector, which is then evenly divided into smaller vector sequences of u_{out} size. Then, each of the evenly divided vectors, $\boldsymbol{w}$, including *don't care* bits is encoded to be a small vector $\boldsymbol{c}$ (of u_{in} size) without any *don't care* bits. Through the XOR gates, each compressed vector $\boldsymbol{c}$ is decoded to be $\boldsymbol{w}'$ consisting of correct *care* bits and randomly filled *don't care* bits with respect to $\boldsymbol{w}$. The structure of XOR gates is fixed during the entire process and, as depicted in Figure 3, can be described as a binary matrix $\boldsymbol{A} \in \{0,1\}^{u_{out} \times u_{in}}$ over **Galois Field** with two elements, $GF(2)$, using the connectivity information between the input vector $\boldsymbol{c} \in \{0,1\}^{u_{in}}$ (compressed weights) and $\boldsymbol{w} \in \{0, x, 1\}^{u_{out}}$. Note that $\boldsymbol{A}$ is pre-determined and simply designed in a way that each element is randomly assigned to 0 or 1 with the same probability.

We intend to generate a random output vector using a seed vector $\boldsymbol{c}$ while targeting as many *care* bits of $\boldsymbol{w}$ as possible. In order to increase the number of successfully matched *care* bits, XOR gates should be able to generate various random outputs. In other words, when the sizes of a seed vector and an output vector are given as u_{in} and u_{out} respectively, all possible $2^{u_{in}}$ outputs need to be well distributed in $2^{u_{out}}$ solution space.

Before discussing how to choose u_{in} and u_{out}, let us first study how to find a seed vector $\boldsymbol{c}$, given $\boldsymbol{w}$. As shown in Figure 3, the overall operation can be expressed by linear equations $\boldsymbol{Ac} = \boldsymbol{w}$ over $GF(2)$. Note that linear equations associated with *don't care* bits in $\boldsymbol{w}$ can be ignored, because the XOR decompressor can produce any bits in the locations of *don't care* bits. By deleting unnecessary linear equations, the original equation form can be simplified (e.g., $\boldsymbol{A'c} = \boldsymbol{w'}$ with only 4 *care* bits on the right side of Figure 3). Given the pruning rate S, $\boldsymbol{w}$ contains $u_{out} \times (1 - S)$ *care* bits on average. Assuming that $u_{out} \times (1 - S)$ equations are independent and non-trivial, the required number of seed inputs (u_{in}) can be as small as $u_{out} \times (1 - S)$, wherein the compression ratio

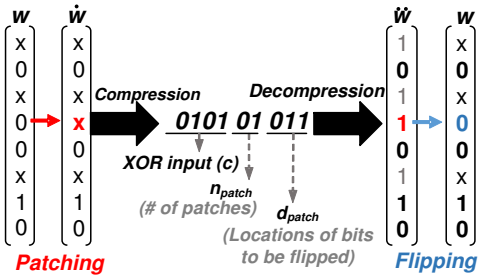

Figure 4: For every $\boldsymbol{w}$, additional n_{patch} and d_{patch} are attached to match all *care* bits. In the example of Figure 3, $\boldsymbol{A}$ is as small as an (8×4) matrix, and the patch data sequence is longer than an XOR input sequence. As explained later in details, however, data for patches is reduced at a faster rate for increasing size of $\boldsymbol{A}$.

u_{out}/u_{in} becomes $1/(1-S)$. As a result, higher pruning rates lead to higher compression ratios. However, note that the linear equations may not have a corresponding solution when there are too many 'local' *care* bits or there are conflicting equations for a given vector $\boldsymbol{w}$.

2.2 Extra Patches for Lossless Compression

In order to keep our proposed SQNNs representation lossless, we add extra bits to correct unavoidable errors, i.e., patching. An unsolvable $\boldsymbol{A}'\boldsymbol{c} = \boldsymbol{w}'$ implies that the XOR random number generator cannot produce one or more matched *care* bits of $\boldsymbol{w}$. To resolve such an occasion, we can replace one or more *care* bits of $\boldsymbol{w}$ with *don't care* bits to remove conflicting linear equations within $\boldsymbol{A}'\boldsymbol{c} = \boldsymbol{w}'$, as depicted in Figure 4. We record the locations of replacements as d_{patch} which can be used to recover the original *care* bits of $\boldsymbol{w}$ by *flipping* the corresponding bits during decompression. For every $\boldsymbol{w}$, n_{patch} indicates the number of replacements for each $\boldsymbol{c}$. Since n_{patch} is always scanned prior to decompressing $\boldsymbol{c}$, the same number of bits is reserved to represent n_{patch} for all compressed vectors in order to maintain a regular compressed format. On the other hand, the size of d_{patch} can be different for each $\boldsymbol{w}$ (overall parallelism is not disrupted by different d_{patch} sizes as flipping occurs infrequently).

At the expense of n_{patch} and d_{patch}, our compression technique can reproduce all *care* bits of $\boldsymbol{w}$ and, therefore, does not affect accuracy of DNN models and obviates retraining. In sum, the compressed format includes 1) $\boldsymbol{c}_{1...l} \in \{0,1\}^{u_{in}}$ ($l = \lceil \frac{mn}{u_{out}} \rceil$) compressed from a weight matrix $\boldsymbol{W}_i^q \in \{0, x, 1\}^{m \times n}$ through $\boldsymbol{A} \in \{0,1\}^{u_{out} \times u_{in}}$, 2) n_{patch}, and 3) d_{patch}. Hence, the resulting compression ratio r is

$$r = \frac{mn}{(\frac{u_{in}}{u_{out}}mn + l\lceil \lg \max(\boldsymbol{p}) \rceil + \sum_{i=1}^{l} p_i \lceil \lg u_{out} \rceil)}, \quad (1)$$

where p_i is the i^{th} n_{patch} and $\boldsymbol{p} = \{p_1, p_2, ..., p_l\}$. Improving r is enabled by increasing u_{out}/u_{in} and decreasing the amount of patches. We introduce a heuristic patch-searching algorithm to reduce the number of patches while also optimizing u_{in} and u_{out}.

2.3 Experiments Using Synthetic Data

An exhaustive search of patches requires exponential-time complexity even though such a method minimizes the number of patches. Algorithm 1 is a heuristic patch-searching algorithm that uses masking information $\boldsymbol{m} \in \{0,1\}^{u_{out}}$ corresponding to $\boldsymbol{w}$ in $\boldsymbol{W}$. The algorithm incrementally enlarges the equation of $\boldsymbol{A}'\boldsymbol{c} = \boldsymbol{w}'$ by including a *care* bit only when the enlarged equation is still solvable. Note that make_rref() in Algorithm 1 generates a reduced row-echelon form to quickly verify that the linear equations are solvable. If adding a certain *care* bit makes the equations unsolvable, then a *don't care* bit takes its place, and n_{patch} and d_{patch} are updated accordingly. Although Algorithm 1 yields more replacement of *care* bits than an exhaustive search (by up to 10% from our extensive experiments), our simple algorithm has time complexity of $O(u_{out})$, which is much faster.

Algorithm 1: Patch-Searching Algorithm

input : masking vector $\boldsymbol{m} \in \{0,1\}^{u_{out}}$, weight vector $\boldsymbol{w} \in \{0,x,1\}^{u_{out}}$, matrix $\boldsymbol{A}^{u_{out} \times u_{in}}$
output : n_{patch}, d_{patch}, $\boldsymbol{c}$

```
mat = empty matrix which column size is u_in + 1
for i = 1 to u_out do
    if m[i] is 1 then                                   // If a parameter is not pruned
        Append a row (A_{i,1}, ...., A_{i,u_in}, w_i) to mat
        rref = make_rref(mat)
        if rref.is_solved() is False then
            Remove the last row of mat from mat
        end if
    end if
end for
Solve linear equations using mat to find c
Compute ẅ = Ac
Compare ẅ with w to produce n_patch and d_patch
Return n_patch, d_patch, c
```

To investigate the compression capability of our proposed scheme, we evaluate a large random weight matrix of 10,000 elements where each element becomes a *don't care* bit with the probability of 0.9 (=sparsity or pruning rate). If an element is a *care* bit, then a 0 or 1 is assigned with the same probability. Notice that randomness of locations in *don't care* bits is a feature of fine-grained pruning methods and assignment of 0 or 1 to weights with the same probability is obtainable using well-balanced quantization techniques [1, 21].

When u_{in} is fixed, the optimal u_{out} maximizes the memory reduction offered by Algorithm 1. Figure 5a plots the corresponding memory reduction (=$1 - r^{-1}$) from $\boldsymbol{W}_i^q$ on the right axis and the amount of $\boldsymbol{c}$ and n_{patch} + d_{patch} on the left axis across a range of u_{out} values when $u_{in} = 20$. From Figure 5a, it is clear that there exists a trade-off between the size of $\boldsymbol{c}$ and the sizes of n_{patch} and d_{patch}. Increasing u_{out} rapidly reduces $\boldsymbol{c}$ while n_{patch} and d_{patch} grow gradually. The highest memory reduction ($\approx$ 0.83) is achieved when u_{out} is almost 200, which agrees with the observation that maximum compression is constrained by the relative number of *care* bits [32]. Consequently, the resulting compression ratio approaches $1/(1-S)$, where S is the sparsity.

Given the relationship above, we can now optimize u_{in}. Figure 5b compares memory reduction for various u_{out} across different values of u_{in}. The resulting trend suggests that higher u_{in} yields more memory reduction. This is because increasing the number of bits used as seed values for the XOR-gate random number generator enables a larger solution space and, as a result, fewer d_{patch} are needed as u_{in} increases. The large solution space is especially useful when *don't care* bits are not evenly distributed throughout $\boldsymbol{W}^q$. Lastly, u_{in} is constrained by the maximum computation time available to run Algorithm 1.

Figure 5c presents the relationship between pruning rate S and memory reduction when $u_{in} = 20$ and sweeping S. Since high pruning rates translate to fewer *care* bits and relatively fewer d_{patch}, Figure 5c confirms that memory reduction approaches S as S increases. In other words, maximizing pruning rate is key to compressing quantized weights with high compression ratio. In comparison, ternary quantization usually induces a lower pruning rate [38, 24]. Our proposed representation is best implemented by pruning first to maximize pruning rate and then quantizing the weights.

3 Experiments on various SQNNs

In this section, we show experimental results of the proposed representation for four popular datasets: MNIST, ImageNet [31], CIFAR10 [17], and Penn Tree Bank [27]. Though the compression ratio ideally reaches $1/(1-S)$, the actual results may not, because *don't care* bits can be less evenly distributed than the synthetic data we used for Section 2. Hence, we suggest several additional techniques in this section to handle uneven distributions.

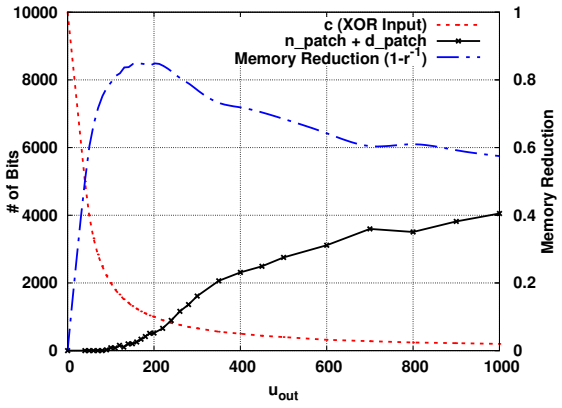

(a) Memory reduction by applying Algorithm 1 to a random weight matrix with 10,000 elements with various u_{out} (pruning rate S=0.9, u_{in}=20)

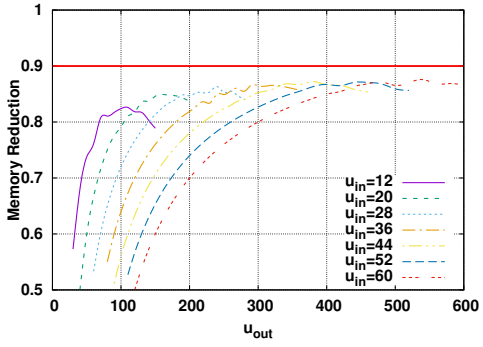

(b) Memory reduction using various u_{in}. Pruning rate is 0.90 and u_{in} ranges from 12 to 60. Each line is stopped when the memory reduction begins to fall.

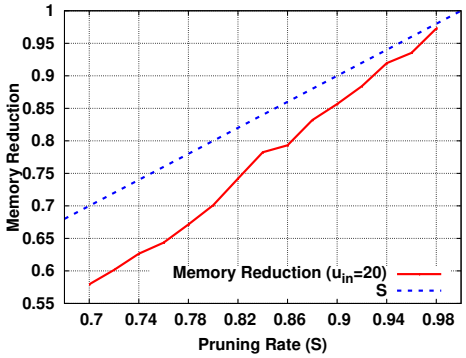

(c) Graphs of memory reduction using u_{in}=20 (red line) and S (blue line). The gap between those two graphs is reduced with higher pruning rate.

Figure 5: Experimental results using synthetic data and Algorithm 1

Table 1: Descriptions of models to be compressed by our proposed method. The model accuracy after parameter pruning and quantization is obtained by a binary-index factorization [23] and alternating multi-bit quantization [34].

Target Model			Pre-trained	Pruning and Quantization		
Model	DataSet	Size	Acc.	S	n_q-bit	Acc.
LeNet5 (FC1)	MNIST	800×500	99.1%	0.95	1-bit	99.1%
AlexNet (FC5, FC6)	ImageNet	9K×4K (FC5) 4K×4K (FC6)	80.3% (T5) 57.6% (T1)	0.91	1-bit	79.6% (T5) 55.9% (T1)
ResNet32	CIFAR10	460.76K	92.5%	0.70	2-bit	91.6%
LSTM	PTB	6.41M	89.6 PPW	0.60	2-bit	93.9 PPW

3.1 Experimental Results

Weights are pruned by the mask layer generated by binary-index matrix factorization [23] after pre-training, and then retrained. Quantization is performed by following the technique proposed in [22] and [16], where quantization-aware optimization is performed based on the quantization method from [34]. The number of bits per weight required by our method is compared with the case of n_q-bit quantization with an additional 1-bit indicating pruning index (e.g., ternary quantization consists of 1-bit quantization and 1-bit pruning indication per weight).

We first tested our representation using the LeNet-5 model on MNIST. LeNet-5 consists of two convolutional layers and two fully-connected layers [9, 22]. Since the FC1 layer dominates the

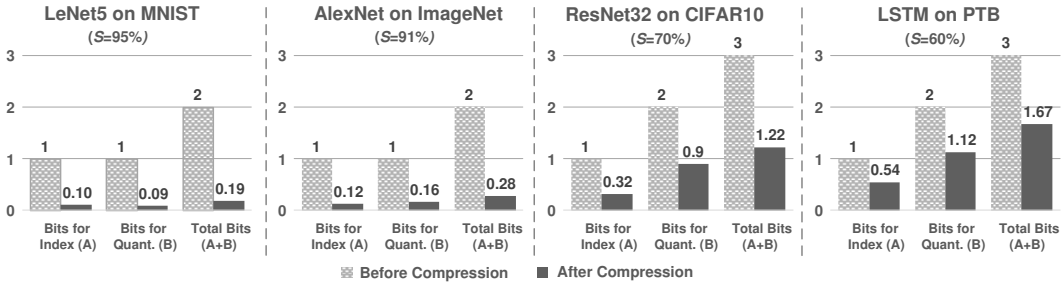

Figure 6: The number of bits to represent each weight for the models in Table 1 using our proposed SQNNs format. (A) means the number of bits for index (compressed by binary-index matrix factorization introduced in [23]). (B) indicates the number of bits for quantization by our proposed compression technique. Overall, we gain additional 2-11$\times$ memory footprint reduction according to sparsity.

memory footprint (93%), we focus only on the FC1 layer whose parameters can be pruned by 95%. With our proposed method, the FC1 layer is effectively represented by only 0.19 bits per weight, which is $11\times$ smaller than ternary quantization, as Figure 6 shows. We also tested our proposed compression techniques on large-scale models and datasets, namely, AlexNet [18] on the ImageNet dataset. We focused on compressing FC5 and FC6 fully-connected layers occupying $\sim$90% of the total model size for AlexNet. Both layers are pruned by a pruning rate of 91% [9] using binary-index matrix factorization [23] and compressed by 1-bit quantization. The high pruning rate lets us compress the quantized weights by $\sim$ 7$\times$. Overall, FC5 and FC6 layers for AlexNet require only 0.28 bits per weight, which is substantially less than 2 bits per weight required by ternary quantization.

We further verify our compression techniques using ResNet32 [12] on the CIFAR10 dataset with a baseline accuracy of 92.5%. The model is pruned and quantized to 2 bits, reaching 91.6% accuracy after retraining. Further compression with our proposed SQNN format yields 1.22 bits per weight, while 3 bits would be required without our proposed compression techniques.

An RNN model with one LSTM layer of size 300 [34] on the PTB dataset, with performance measured by using Perplexity Per Word, is compressed by our representation. Note that the embedding and softmax matrices usually take a major memory footprint because of increasing vocabulary size in a neural language model wherein these two matrices have several distinguished properties compared with general weight matrices [4]. In particular, skewed word frequencies in the vocabulary cause inconsistently distributed *don't care* bits inside the embedding and softmax matrices. In the experiment, we compress the embedding and softmax matrices leveraging the randomness in the LSTM layer by shuffling the quantized-weights using an *interleaving* algorithm. The resulting compressed model, with pruning and 2-bit quantization, requires only 1.67 bits per weight.

For various types of layers, our proposed technique, supported by weight sparsity, provides additional compression over ternary quantization. Compression ratios can be further improved by using more advanced pruning and quantization methods (e.g., [33, 8]) since the principles of our compression methods do not rely on the specific pruning and quantization methods used.

3.2 Techniques to Reduce n_{patch}

If u_{out} is large enough, patching overhead is not supposed to disrupt the parallel decoding, ideally. However, even for large u_{out}, when the nonuniformity of pruning rates is observed over a wide range within a matrix, especially with lower pruning rates, n_{patch} may considerably increase. Large n_{patch}, then, leads to not only degraded compression ratio compared with synthetic data experiments, but also deteriorated parallelism in the decoding process. The following techniques can be considered to reduce n_{patch}.

Blocked n_{patch} Assignment: The compression ratio r in the Eq. (8) of Section 3.2 is affected by the maximum of $\{p_1, p_2, ..., p_l\}$. Note that a particular vector $\boldsymbol{w}$ may have an exceptionally large number of *care* bits. In such a case, even if a quantized matrix $\boldsymbol{W}^q$ consists of mostly *don't care* bits and few patches are needed, all of the compressed vectors $\boldsymbol{c}$ must employ a large number of

bits to track the number of patches. To mitigate such a problem and enhance the compression ratio r, we divide a binary matrix $\boldsymbol{W}^q$ into several blocks, and then $\max(\boldsymbol{p})$ is obtained in each block independently. Different n_{patch} is assigned to each block to reduce the overall n_{patch} data size.

Minimizing n_{patch} for Small u_{in}: One simple patch-minimizing algorithm is to list all possible $2^{u_{in}}$ inputs (for $\boldsymbol{c}$) and corresponding $\boldsymbol{w}'$ outputs through $\boldsymbol{A}$ on memory and find a particular $\boldsymbol{c}$ that minimizes the number of patches. At the cost of high space complexity and memory consumption, such an exhaustive optimization guarantees minimized n_{patch}. u_{in} below 30 is a practical value.

Interleaver: We can occasionally observe that a large group of weights are pruned or unpruned altogether because of unique properties of embedding and softmax layers distinguished from typical layers. Interleaver and deinterleaver, widely used in digital communications [29], are useful for such uneven distributions of *don't care* bits. Interleaver intermixes weights in a random manner and deinterleaver recovers the original locations of weights. Designing interlevers and deinterleavers with low encoding/decoding complexity for model compression would be an interesting research topic.

4 Related Works and Comparison

In this section, we introduce two previous approaches to represent sparse matrices. Table 2 describes CSR format, Viterbi-based index format, and our proposed format..

Compressed Sparse Row(CSR): Deep compression [11] utilizes the Compressed Sparse Row (CSR) format to reduce memory footprint on devices. Unfortunately, CSR formats present irregular data structures not readily supported by highly parallel computing systems such as CPUs and GPUs [21]. Due to uneven sparsity among rows, computation time of algorithms based on CSR is limited by the least sparse row [37], as illustrated in Figure 2. Although [10] suggested hardware support via a large buffer to improve load balancing, performance is still determined by the lowest pruning rate of a particular row. In contrast, our scheme provides a perfectly structured format of weights after compression such that high parallelism is maintained.

Viterbi Approaches: Viterbi-based compression [21, 1] attempts to compress pruning-index data and quantized weights with a fixed compression ratio using *don't care* bits, similar to our approach. Quantized weights can be compressed by using the Viterbi algorithm to obtain a sequence of inputs to be fed into Viterbi encoders (one bit per cycle). Because only one bit is accepted for each Viterbi encoder, only an integer number (=number of Viterbi encoder outputs) is permitted as a compression ratio, while our proposed scheme allows any rational numbers (=u_{out}/u_{in}).

Because only one bit is used as inputs for Viterbi encoders, Viterbi-based approaches require large hardware resources. For example, if a memory allows 1024 bits per cycle of bandwidth, then 1024 Viterbi encoders are required, where each Viterbi encoder entails multiple Flip-Flops to support sequence detection. On the other hand, our proposed scheme is resource-efficient to support large memory bandwidth because Flip-Flops are unnecessary and increasing u_{in} is only limited by time complexity of Algorithm 1.

5 Conclusion

This paper proposes a compressed representation for Sparse Quantized Neural Networks based on an idea used for test-data compression. Through XOR gates and solving linear equations, we can remove most *don't care* bits and a quantized model is further compressed by sparsity. Since our representation provides a regular compressed-weight format with fixed and high compression ratios, SQNNs enable not only memory footprint reduction but also inference performance improvement due to inherently parallelizable computations.

References

[1] D. Ahn, D. Lee, T. Kim, and J.-J. Kim. Double Viterbi: Weight encoding for high compression ratio and fast on-chip reconstruction for deep neural network. In *International Conference on Learning Representations (ICLR)*, 2019.

Table 2: Comparisons of CSR, Viterbi, and our proposed representation. For all of these representation schemes, compression ratio is upper-bounded by sparsity.

	CSR Format	Viterbi-based Compr.	Proposed
Encryption	No	Yes	Yes
Load Balance	Uneven	Even	Even
Decoding Rate	Variable	Fixed	Fixed
Parallelism Limited by	Uneven Sparsity	Number of Decoders	Number of Decoders
Memory Access Pattern	Irregular (Gather-Scatter)	Regular	Regular
Compressed Memory Bandwidth	Depends on on-chip Buffer Structure	1 bit/decoder	u_{in} bits/decoder
HW Resource for a Decoder	Large Buffer to improve load balance	XOR gates and Flip-Flops	XOR gates only

[2] S. Anwar, K. Hwang, and W. Sung. Structured pruning of deep convolutional neural networks. *ACM Journal on Emerging Technologies in Computing Systems (JETC)*, 13(3):32, 2017.

[3] I. Bayraktaroglu and A. Orailoglu. Test volume and application time reduction through scan chain concealment. In *Proceedings of the 38th Annual Design Automation Conference*, 2001.

[4] P. Chen, S. Si, Y. Li, C. Chelba, and C.-J. Hsieh. GroupReduce: Block-wise low-rank approximation for neural language model shrinking. In *Advances in Neural Information Processing Systems*, 2018.

[5] M. Courbariaux, Y. Bengio, and J.-P. David. BinaryConnect: Training deep neural networks with binary weights during propagations. In *Advances in Neural Information Processing Systems*, pages 3123–3131, 2015.

[6] M. Denil, B. Shakibi, L. Dinh, N. De Freitas, et al. Predicting parameters in deep learning. In *Advances in neural information processing systems*, pages 2148–2156, 2013.

[7] I. Goodfellow, Y. Bengio, and A. Courville. *Deep Learning*. MIT Press, 2016. `http://www.deeplearningbook.org`.

[8] Y. Guo, A. Yao, and Y. Chen. Dynamic network surgery for efficient DNNs. In *Advances in Neural Information Processing Systems*, 2016.

[9] S. Han, J. Pool, J. Tran, and W. J. Dally. Learning both weights and connections for efficient neural networks. In *Advances in Neural Information Processing Systems*, pages 1135–1143, 2015.

[10] S. Han, X. Liu, H. Mao, J. Pu, A. Pedram, M. A. Horowitz, and W. J. Dally. EIE: efficient inference engine on compressed deep neural network. In *Proceedings of the 43rd International Symposium on Computer Architecture*, pages 243–254, 2016.

[11] S. Han, H. Mao, and W. J. Dally. Deep compression: Compressing deep neural networks with pruning, trained quantization and Huffman coding. In *International Conference on Learning Representations (ICLR)*, 2016.

[12] K. He, X. Zhang, S. Ren, and J. Sun. Deep residual learning for image recognition. *2016 IEEE Conference on Computer Vision and Pattern Recognition (CVPR)*, pages 770–778, 2016.

[13] Y. He, X. Zhang, and J. Sun. Channel pruning for accelerating very deep neural networks. In *Proceedings of the IEEE International Conference on Computer Vision*, pages 1389–1397, 2017.

[14] I. Hubara, M. Courbariaux, D. Soudry, R. El-Yaniv, and Y. Bengio. Quantized neural networks: training neural networks with low precision weights and activations. *arXiv:1609.07061*, 2016.

[15] M. C. Jonathan Frankle. The lottery ticket hypothesis: Finding sparse, trainable neural networks. In *International Conference on Learning Representations (ICLR)*, 2019.

[16] P. Kapoor, D. Lee, B. Kim, and S. Lee. Computation-efficient quantization method for deep neural networks, 2019. URL `https://openreview.net/forum?id=SyxnvsAqFm`.

[17] A. Krizhevsky. Learning multiple layers of features from tiny images. Technical report, 2009.

[18] A. Krizhevsky, I. Sutskever, and G. E. Hinton. Imagenet classification with deep convolutional neural networks. In F. Pereira, C. J. C. Burges, L. Bottou, and K. Q. Weinberger, editors, *Advances in Neural Information Processing Systems 25*, pages 1097–1105. Curran Associates, Inc., 2012.

[19] Y. LeCun, J. S. Denker, and S. A. Solla. Optimal brain damage. In *Advances in Neural Information Processing Systems*, pages 598–605, 1990.

[20] D. Lee and B. Kim. Retraining-based iterative weight quantization for deep neural networks. *arXiv:1805.11233*, 2018.

[21] D. Lee, D. Ahn, T. Kim, P. I. Chuang, and J.-J. Kim. Viterbi-based pruning for sparse matrix with fixed and high index compression ratio. In *International Conference on Learning Representations (ICLR)*, 2018.

[22] D. Lee, P. Kapoor, and B. Kim. Deeptwist: Learning model compression via occasional weight distortion. *arXiv:1810.12823*, 2018.

[23] D. Lee, S. J. Kwon, P. Kapoor, B. Kim, and G.-Y. Wei. Network pruning for low-rank binary indexing. *arXiv:1905.05686*, 2019.

[24] F. Li and B. Liu. Ternary weight networks. *arXiv:1605.04711*, 2016.

[25] H. Li, A. Kadav, I. Durdanovic, H. Samet, and H. P. Graf. Pruning filters for efficient convnets. In *International Conference on Learning Representations*, 2017.

[26] H. Mao, S. Han, J. Pool, W. Li, X. Liu, Y. Wang, and W. J. Dally. Exploring the regularity of sparse structure in convolutional neural networks. *arXiv preprint arXiv:1705.08922*, 2017.

[27] M. Marcus, G. Kim, M. A. Marcinkiewicz, R. MacIntyre, A. Bies, M. Ferguson, K. Katz, and B. Schasberger. The penn treebank: Annotating predicate argument structure. In *Proceedings of the Workshop on Human Language Technology*, HLT '94, pages 114–119, Stroudsburg, PA, USA, 1994. Association for Computational Linguistics. ISBN 1-55860-357-3. doi: 10.3115/1075812.1075835. URL `https://doi.org/10.3115/1075812.1075835`.

[28] D. Molchanov, A. Ashukha, and D. P. Vetrov. Variational dropout sparsifies deep neural networks. In *International Conference on Machine Learning (ICML)*, pages 2498–2507, 2017.

[29] R. H. Morelos-Zaragoza. *The art of error correcting coding*. John Wiley & Sons, 2nd edition, 2006.

[30] M. Rastegari, V. Ordonez, J. Redmon, and A. Farhadi. XNOR-Net: Imagenet classification using binary convolutional neural networks. In *ECCV*, 2016.

[31] O. Russakovsky, J. Deng, H. Su, J. Krause, S. Satheesh, S. Ma, Z. Huang, A. Karpathy, A. Khosla, M. Bernstein, A. C. Berg, and L. Fei-Fei. ImageNet Large Scale Visual Recognition Challenge. *International Journal of Computer Vision (IJCV)*, 115(3):211–252, 2015. doi: 10.1007/s11263-015-0816-y.

[32] N. A. Touba. Survey of test vector compression techniques. *IEEE Design & Test of Computers*, 23: 294–303, 2006.

[33] P. Wang, X. Xie, L. Deng, G. Li, D. Wang, and Y. Xie. HitNet: Hybrid ternary recurrent neural network. In *Advances in Neural Information Processing Systems*, 2018.

[34] C. Xu, J. Yao, Z. Lin, W. Ou, Y. Cao, Z. Wang, and H. Zha. Alternating multi-bit quantization for recurrent neural networks. In *International Conference on Learning Representations (ICLR)*, 2018.

[35] J. Ye, X. Lu, Z. Lin, and J. Z. Wang. Rethinking the smaller-norm-less-informative assumption in channel pruning of convolution layers. *arXiv preprint arXiv:1802.00124*, 2018.

[36] J. Yu, A. Lukefahr, D. Palframan, G. Dasika, R. Das, and S. Mahlke. Scalpel: Customizing DNN pruning to the underlying hardware parallelism. In *Proceedings of the 44th Annual International Symposium on Computer Architecture*, pages 548–560, 2017.

[37] X. Zhou, Z. Du, Q. Guo, S. Liu, C. Liu, C. Wang, X. Zhou, L. Li, T. Chen, and Y. Chen. Cambricon-s: Addressing irregularity in sparse neural networks through a cooperative software/hardware approach. In *2018 51st Annual IEEE/ACM International Symposium on Microarchitecture (MICRO)*, pages 15–28. IEEE, 2018.

[38] C. Zhu, S. Han, H. Mao, and W. J. Dally. Trained ternary quantization. In *International Conference on Learning Representations (ICLR)*, 2017.

[39] M. Zhu and S. Gupta. To prune, or not to prune: exploring the efficacy of pruning for model compression. *CoRR*, abs/1710.01878, 2017.